Mechatronics 21 (2011) 490–500

Contents lists available at ScienceDirect

Mechatronics

journal homepage: www.elsevier.com/locate/mechatronics

How to achieve the huggable behavior of the social robot Probo? A reflection on the actuators

Kristof Goris [a,b,*], Jelle Saldien [a], Bram Vanderborght [a], Dirk Lefeber [a]

[a] Vrije Universiteit Brussel, Robotics & Multibody Mechanics Research Group, Pleinlaan 2, 1050 Brussel, Belgium
[b] Group T – Leuven Engineering College (Association K.U. Leuven), A.Vesaliusstraat 13, 3000 Leuven, Belgium

ARTICLE INFO

Article history:
Received 3 May 2010
Accepted 10 January 2011
Available online 12 February 2011

Keywords:
Social robot
Compliant actuation
Huggable
Safety
Human–robot interaction (HRI)

ABSTRACT

Most robots have a mechanical look or are covered with plastic or metallic shells. Their actuators are stiff which gives them not only an unnatural look, but also an unnatural touch. The goal of the huggable robot Probo is to serve as robotic research platform for human–robot interaction (HRI) studies with a special focus on children. Since not only cognitive interaction, but also physical interaction is targeted a new mechatronic design must be developed. To give Probo a huggable and safe behavior a new set of actuators is developed together with a triple layered protection cover which is presented in this paper. Probo's soft touch is introduced, on the one side by use of novel passive compliant actuators, Compliant Bowden Cable Driven Actuators (CBCDAs), and on the other side by combining custom made servo motors, Non Back Drivable Servos (NBDSs), with flexible components and materials such as springs, silicon and foam. The working principle of the novel CBCDA is extensively described, together with experiments in order to determine its level of compliance and its bandwidth.

1. Introduction

The overall trend in robotics is that robots will work more frequently with humans. For a good collaboration a good communication between the robot and human is necessary. To communicate in a proper manner the robots can be equipped with some human-like traits, for instance, facial expressions and gestures. According to Mehrabian [1], most of our communication goes over non-verbal means, like facial expression and gestures. When a robot has these capabilities as well, one can speak of social robots. The face is the most important element to express social cues and different projects focus on the face like eMuu [2], Feelix [3], iCat [4] and Kismet [5]. Robots that also include gestures by moving the whole upper body, including arms and hands, are Leonardo [6], Infanoid [7], Kaspar [8], Robovie-IV [9], WE-4RII [10] and Nexi [11]. ASIMO [12], QRIO [13], Kobian [14] and iCub [15] are complete humanoids that use their full body to interact with the humans and the environment. Paro [16], Robota [17], Keepon [17] and the Huggable [18] are social robots that especially focus on robot assisted therapy (RAT). These social robots place the human central during human–robot interaction instead of the robot itself. The research field that studies this is called human–robot interaction (HRI) and is a multidisciplinary field with contributions from human–computer interaction, artificial intelligence, robotics, natural language understanding, and social sciences. This new research area requires proper designed mechatronic systems.

Over the recent years different social robots have been built and some of them are commercialized. Aibo [19] and Pleo are intelligent companions that appeared on the market embodied as robot pets. Despite the potential this was not a great success yet. Only the cheap robotic toys like Furby and the WowWee robots were able to have commercial success. Nonetheless are these robotic toys contributing to the future market for social robots. Results from research will be gradually implemented in these toys to enhance the interactions with the user. Most of the social robots now are used for HRI studies.

Our huggable robot Probo's purpose is to serve as a multidisciplinary research platform for HRI focused on children. In most social robots is focussed on vision and audio, the study of tactile communication has often been neglected [10] with exceptions as Paro [16], Leonardo [6], the Huggable [20] and Robovie-iv [9]. Probo aims besides cognitive interaction also physical interaction. This desire leads to other design requirements that need to be fulfilled. For instance, safety aspects are one of the most important issues during physical HRI. To achieve these goals, a concept of a new child-friendly artificial creature, called Probo has been developed. Fig. 1 shows a section view of the real prototype of Probo. A close up of Probo's robotic head is presented in Fig. 2. The main difference with other social robots is the use of compliant actuators,

* Corresponding author at: Vrije Universiteit Brussel, Robotics & Multibody Mechanics Research Group, Pleinlaan 2, 1050 Brussel, Belgium.
E-mail addresses: kristof.goris@vub.ac.be, kristof.goris@groept.be (K. Goris).
URL: http://probo.vub.ac.be (K. Goris).

0957-4158/$ - see front matter © 2011 Elsevier Ltd. All rights reserved.
doi:10.1016/j.mechatronics.2011.01.001

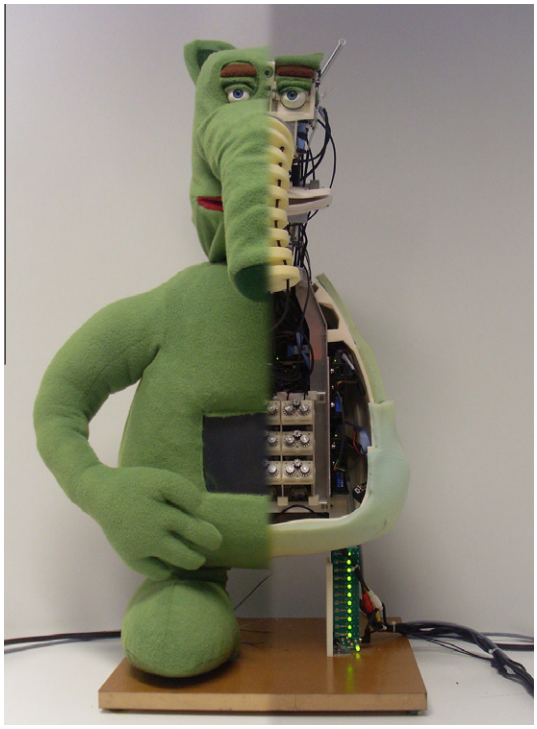

Fig. 1. A section view of the real Probo prototype.

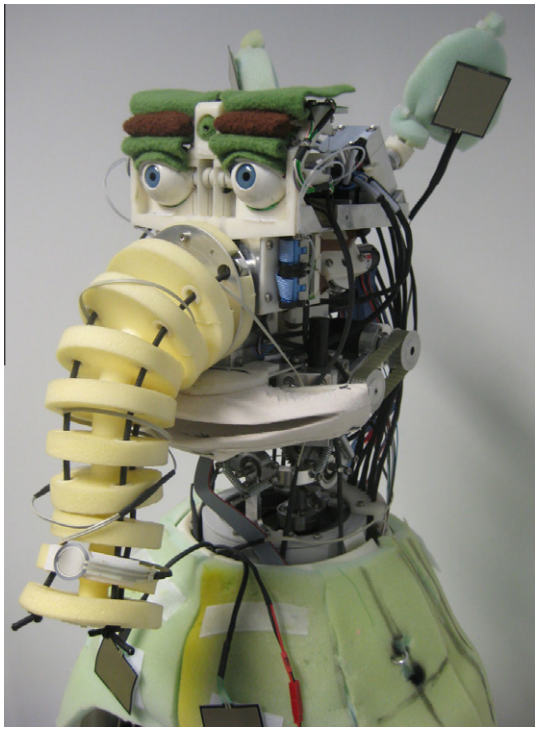

Fig. 2. A picture of the uncovered robotic head of Probo.

lightweight design and the fur to achieve intrinsically safety and providing a soft touch and a huggable appearance.

To achieve a modular robot systems that in the future can easily be modified or extended, a modular construction approach has been opted in both hardware as software. The systems are designed in such a way that they can work independently. Some of the designed (sub)systems are used multiple times in different assemblies to perform a variety of tasks. For instance, the actuators described in Section 2 are used to actuate joints in systems such as the eyes and eyebrows. A schematic overview of the actual Probo prototype hardware architecture is presented in Fig. 3. This scheme presents the internal hardware of Probo with exclusion of the perceptual sensory. In the scheme can be seen that Probo consists of different functional systems such as the eye-system, the eyebrow-system, the ear-system, the mouth-system, the trunk-system and the neck-system. These are presented by the light-gray columns, and are extensively described in other work of the authors. All these systems have the same function, namely the creation of motions and expressions. In order to do so, these systems are built out of different structural mechanical assemblies, including actuated parts, actuators, motor controllers, wires, sensors, etc. These subsystems can be grouped in different layers. Each layer describes the main function of the grouped subsystems. There are five layers described as:

- Motion and Expression layer
- Actuation layer
- Low Level Drive layer
- Supply layer
- High Level Drive layer

One notices that the actuation layer is mostly filled with the NBDS and CBCDA actuation principle. The neck-system is powered by three direct drives in parallel with a spring mechanism. These three neck motions require powerful actuators, since the head is the heaviest assembly to move. To reduce the motor size and consequently make the system lighter and safer, a parallel spring mechanism is installed. This paper will focuss on the actuators of Probo.

2. Actuators for Probo

Despite, the ever since desire of building safety into robot systems, the safety nowadays is mostly obtained by keeping humans away from robots. For instance, in industrial environments, the robots are placed in safety cages. However, since more and more robots will be used among humans, these safety aspects have to be built into the system intrinsically. The implementation of safety aspects in robotics gains in interest. Possible approaches to obtain safety are: well-thought designs of light and flexible structures, the use of compliant actuators, appropriate material choices, and fail safe designs. This approach has been followed during the development of Probo. At the same time aspects as soft and flexible materials in combination with compliant actuators, contribute to the huggable and soft behavior of Probo.

Since electrical motors typically deliver relative small torques at high operating speeds, a reduction mechanism (e.g., a gearbox) with high reduction ratio is required to deliver sufficient torques at nominal operating speeds. Unfortunately, these reduction mechanisms introduce disadvantageous side-effects. First of all they introduce a power loss. Secondly, due to the reflected moment of inertia of the gears, the moment of inertia of the output shaft of the system will increase by the square of the reduction ratio. As a consequence, the output shaft gets very stiff. Since the actuators will be used in HRI applications, the high stiffness can lead to undesirable and possible dangerous situations. For instance, during operation, high contact forces can occur between human and robot, and consequently human can get hurt and/or the robot can break down. During a collision, the complete inertia of the robot is felt. To avoid these situations, the current trend in robotics is to make the robots soft or compliant. In case of a collision with a compliant actuated robot, the inertia of the link in collision is decoupled from

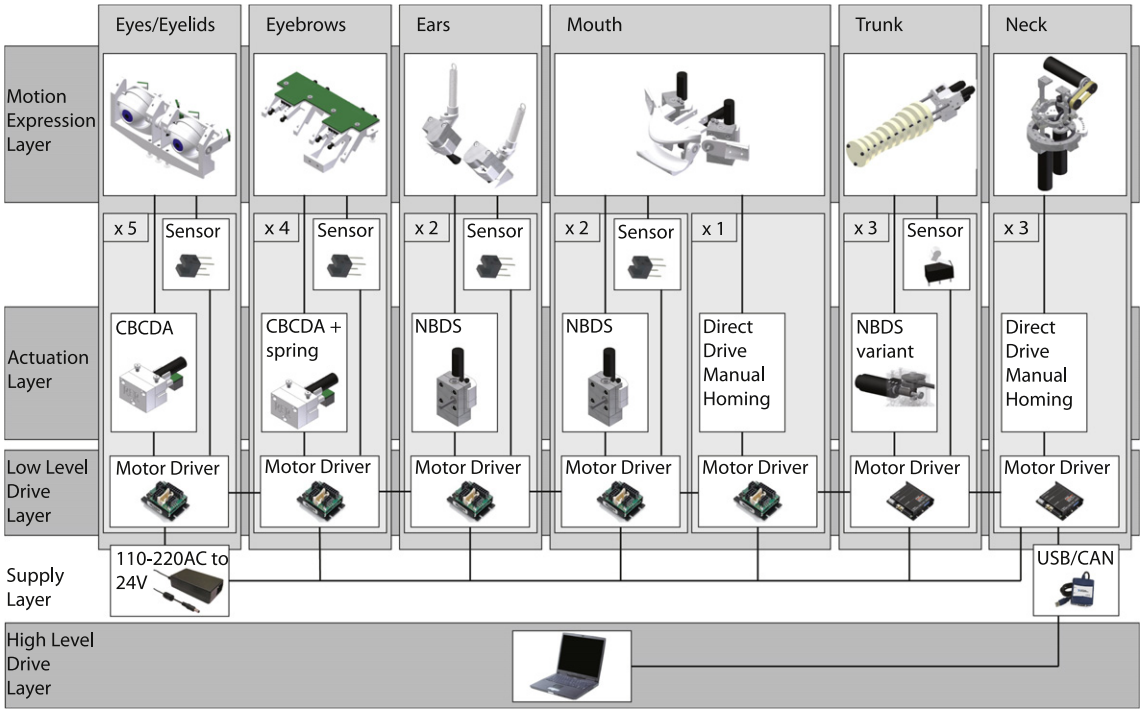

Fig. 3. Schematic overview hardware structure of the Probo prototype.

the rest of the robot [21]. This approach leads to safe and human friendly robots, useful in applications and environments where human and robot have to collaborate.

There are different ways to introduce compliant behavior into a system. It can be obtained by means of design, for instance, by using flexible materials. This kind of compliance is referred to as *passive* compliance. Another way to obtain compliant behavior can by means of control, which is referred to as *active* compliance. Both approaches have their advantages and disadvantages. For instance, the main advantage of a passive compliant system is its inherent *soft touch*, which does not depend on control algorithms. However, at the same time, this inherent compliance makes the control difficult, which generally leads to lower performances in terms of operating speeds and accurate positioning. On the other side, the active compliant system which uses traditionally rigid and stiff actuators introduces less control problems during precise tracking operations. But, the controller must be able to introduce the soft touch at any time. Consequently the soft touch depends on the actuator, sensor and control bandwidth. With Probo's 20 DOFs, complexity, both in hardware and in software design, will increase fast when all joints have to be equipped with torque sensors in order to introduce the compliance actively. Moreover since the compliance has to be intrinsically embedded in Probo, to ensure a soft touch at all times, there has been chosen to design the Probo prototype by use of passive compliance.

In [22] *Ronald Van Ham* presents a review of different compliant actuator designs. Basically there are two sorts of conventional (includes hydraulic, pneumatic, and electric) compliant actuators. The first groups all actuators with a predefined or fixed compliance. These actuators can be used for force control or in safe HRI applications. The second type of compliant actuators groups all actuators with variable (or also used; controllable, or adjustable) compliance (or its opposite, stiffness). These actuators have an elastic element to store energy, and a way to adapt the compliance (or stiffness). According to *Van Ham* in [22], there are four main ideas to adapt the compliance: (i) by adjustment of the equilibrium position of elastic elements such as springs (e.g., *Series Elastic Actuator (SEA)*[23]); (ii) by an antagonistic setup of two non-linear elastic elements (e.g., antagonistic setup of two pneumatic muscles *(PPAM)* [24], *Variable Stiffness Actuator (VSA)* [25]); (iii) by controlling the flexibility of the compliant element of the system (e.g., *Jack Spring Actuator* [26]); (iv) by controlling mechanically the attaching points of the elastic elements (e.g., *Mechanically Adjustable Compliance and Controllable Equilibrium Position Actuator (MACCEPA)* [27]). Many researchers state that compliant actuators are sufficient to guarantee safety. However, recent work by Haddadin et al. in the scope of the European Framework program *Phriends* negate this statement and propose new insights to introduce safety, based upon impact experiments with the *DLR-Lightweight Robot III* [28]. Simultaneous work of Michaël Van Damme [21] shows that a manipulator powered by pneumatic muscles as compliant actuator can be considered unsafe when under PID control. Reason is that compliant actuators have the ability to store energy and subsequently release suddenly the energy, making it more dangerous. He implemented the *Proxy-based Sliding Mode Control (PSMC)* that besides the tracking control also takes the safety aspect in the control strategy. The springs used in Probo cannot store enough energy to be unsafe and consequently there was no need to implement such a dedicated control strategy. Furthermore the relative low speeds and accelerations of the lightweight ABS with fur covered actuated parts of Probo, leads to insignificant impacts.

Novel non conventional actuators can be developed based on advances in material technology by making use of *smart* materials such as shape memory alloys, electrorheological fluids, electrostrictive and magnetostrictive materials and electroactive polymers. These fields of study will not be described in the scope of the presented work. In general, they are not yet sufficiently developed to be used in Probo as their operation speeds are very low, with time constants in the order of tens of seconds and they generate weak forces [29–31].

Traditional actuators as electrical drives with gearboxes are unsuitable to use in Probo because they are stiff, giving an unnatural hard touch. Two different compliant actuators are developed to cope with this problem, on the one side by use of novel passive

compliant actuators, *Compliant Bowden Cable Driven Actuators (CBCDA)*, and on the other side by combining custom made servo motors, *Non Back Drivable Servo (NBDS)*, with flexible components and materials such as springs, silicon and foam. In both actuators the flexible element plays an essential role since it decouples the inertia of the colliding link with the rest of the robot, reducing the potential damage during impact [21].

2.1. Compliant Bowden Cable Driven Actuators (CBCDA)

2.1.1. Description

The first type of custom actuator used in the Probo prototype is referred to as *Compliant Bowden Cable Driven Actuator (CBCDA)*. The CBCDA is a custom made passive compliant servo motor system which transmits motion over a relative long distance compared to its own size. Fig. 4 shows a typical setup of a CBCDA actuating a joint. The entire system exists of the CBCDA and the actuated part, or joint. The use of the CBCDAs creates the opportunity to group and to isolate the different actuators and to place them anywhere in the robot. That way heat and noise dissipation can be controlled. Furthermore, in the case of Probo, its head can be held light-weighted, since most of the CBCDAs are located in its belly, resulting in a safer design. The compliant characteristic is introduced by both the flexible *Inner Cable* and flexible *Cable Housing*. The combination of an inner cable inside an outer cable housing is referred to as a *Bowden Cable (BC)*.

The main components of a CBCDA used in Probo are a *DC motor*, a pair of *Bowden Cables*, and a set of *pulleys*. Fig. 5 shows a transparent view of the CAD-model to explain the working principle. A geared (with transmission ratio of 67:1) DC brushed *maxon* motor (of 3 W) that is equipped with an incremental encoder (with 128 cpt) drives *Gear 1* on axis A_p and *Gear 1'* on axis A'_p via a *Pinion* gear on axis A_m (input shaft). This is the first transmission. This design provides a compact design, the ease to replace the motor-combination, and the possibility to allow some small mis-alignment errors, this transmission is fundamental in the CBCDA. *Gear 1* and *Gear 1'* are fixed respectively to *Pulley 1* on axis A_p and *Pulley 1'* on A'_p. *Cable 1* and *Cable 1'* are fixed to respectively *Pulley 1* and *Pulley 1'*. During the assembly of the CBCDA, both cables are *pre-wound* several times

Fig. 4. A typical setup of a joint actuated by a CBCDA. The transmission of motion occurs by the inner cable in an outer cable housing over a long distance (the middle part of the cable is trimmed in the Figure).

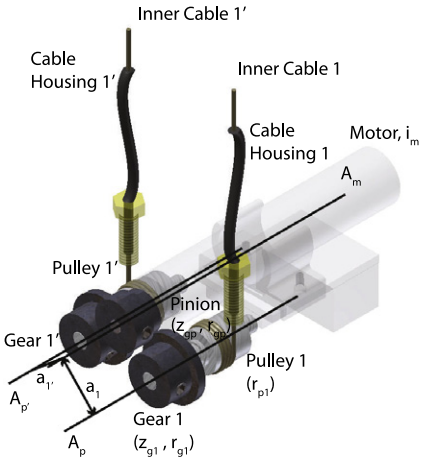

Fig. 5. Transparent views of the CAD-model to explain the working principle of the CBCDA. The motor drives the pulleys. One cable is winded around the pulley while at the same time another one is released from the other pulley.

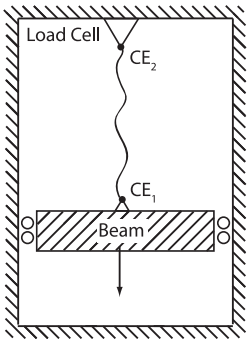

Fig. 6. Setup to determine the stiffness of the cables.

around the pulleys *in opposite direction* as shown in Fig. 5. This can only be done when the *Pinion* gear is removed, by turning *Gear 1 clockwise*, and *Gear 1' anticlockwise*. During normal operation the *Pinion* gear is driven by the motor-combination. When it is turning (e.g., anticlockwise), both pulleys will turn in the opposite direction (so, in the supposed case, clockwise). In the example where the motor turns anticlockwise, *Pulley 1* will turn clockwise and consequently *Inner Cable 1* will be wound further around *Pulley 1*. At the same time *Pulley 1'* will also turn clockwise and consequently *Inner Cable 1'* will be released from *Pulley 1'* since it was already pre-wound during assemblage. The *Inner Cables 1, 1'* are guided through *Cable Housings 1, 1'*. The end points of *Cable Housing 1* and *Cable Housing 1'* are constrained by respectively barrel adjuster S_1 and barrel adjuster S'_1 (colored yellow[1] in Fig. 5). These barrel adjusters are screws which are drilled in such a way that the inner cable can pass through the screw, while the outer cable housing can not pass and consequently is constrained by the screw. When both ends of the outer cable housing of a BC are constrained, a motion can be transmitted by pulling on the inner cable. By winding an inner cable around its pulley, a pull force is generated. Consequently this pull force can be used to *pull* on a lever arm, or to *rotate* a pulley. In the setup presented in Fig. 4, a pair of BCs is used in an antagonistic setup, to actuate the joint.

[1] For interpretation of color in Figs. 1–5, 7, 8, 10–13, 15–19, 21, and 23–29, the reader is referred to the web version of this article.

2.1.2. Compliance of the CBCDA

The compliance of the CBCDA is obtained by both the elasticity (or its opposite, stiffness) of the flexible *inner cable* and the elasticity of the *cable housing*.

To determine the stiffness of the inner cables, samples were pulled, in a mechanical draw bench, until they broke. The experimental setup is displayed in Fig. 6. During the experiments, the *Beam* moved downwards with a constant speed of 100 mm/s. This introduced a tension in the cable, which ends ($CE_1$and CE_2) are fixed to the *Beam* and the *Load Cell*. For each sample, the force displacement characteristic was measured. The mean values of three measurements per type of cable are presented in Fig. 7. Fig. 8 shows a close up of the results in the working area to transmit motions by use of Probo's CBCDAs. The four different types of cable samples differ in material properties. The names are related to the product names. *Guttermann* and *Chinese* are two types of textile yarn or threads. *Nylon* and *Fireline* are wires used as fishing lines. The diameters of the cables are all approximately 0.4 mm and the samples' lengths were 250 mm. As one can see in the figure, the characteristic of the *Fireline* cable has a non-linear behavior in this range.

In a similar way the stiffness of the BCs' outer cables, or cable housings are determined. These cable housings are made out of *SCI scientific commodities' PFA MEDICAL MICRO TUBING* [32]. These flexible hollow tubes are mainly used in medical environment, for instance, as catheters. The used tubes have an inner diameter of 0.56 mm and an outer diameter of 1 mm. In order to become the outer housing of the BC, the PFA tubes are covered by different layers of heat shrink tubes. The total diameter of the outer cable

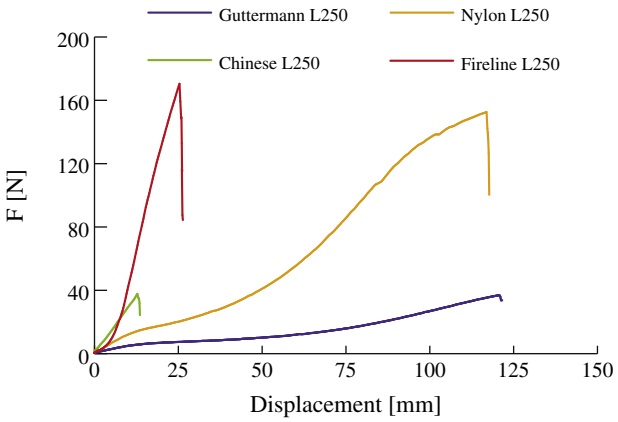

Fig. 7. Force displacement characteristics of four different cable samples with a length of 250 mm.

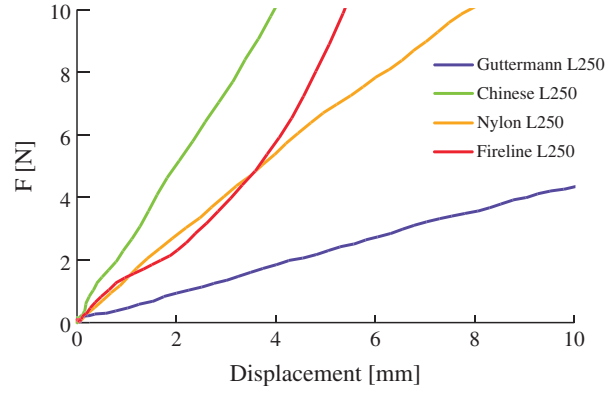

Fig. 8. Detailed view of the force displacement characteristics in the relevant working area.

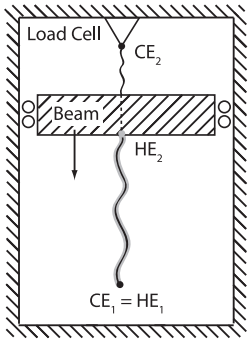

Fig. 9. Setup to determine the stiffness of the BCs.

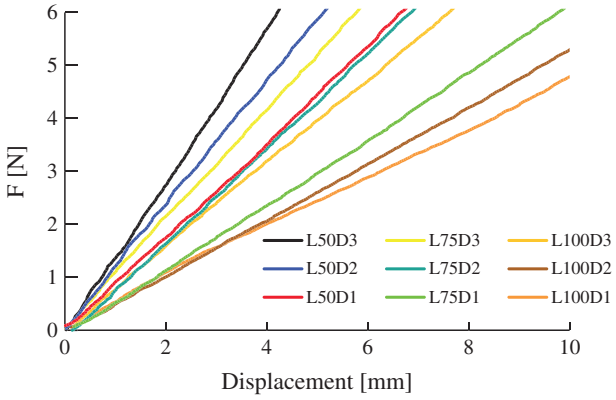

Fig. 10. Force displacement characteristics of different Bowden cable samples.

housing is now increased, and the flexibility has changed as well. By repeating the process of covering the outer cables with additional heating shrink tubes, followed by heating them, different setups of BC housings are manufacturable. These different setups will differ in stiffness. Fig. 10 presents the experimentally measured force displacement characteristics of different samples. The plotted graphs represent the mean values of three experiments with the same sample. The experimental setup is presented in Fig. 9. One of the cable housing's ends (HE_1) was constrained by the *Beam* of the draw bench, while the other end (HE_2) was fixated to the end of the inner cable (CE_2) which was guided by the cable housing. The other end of the inner cable (CE_1) was attached to a *Load Cell*. When the beam moved downwards, the cable housing was pushed together around the inner cable. The related push force was measured by the load cell. The samples' lengths were 50 cm, 75 cm and 100 cm, and the diameter differed according to the number of extra shrink tube covers (1, 2 or 3). As one can see, the measured curves have a linear behavior.

In Probo's CBCDA actuated mechanisms, the *Fireline* cable and various setups of cable housings (they differ in length and in diameter) are used. Due to the non-linear force displacement characteristic of the *Fireline* cable, the stiffness of the entire BC is non-linear in a limited range. Consequently, the system's compliance (or stiffness) can be set when the BCs are used in an antagonistic setup. According to *Van Ham*'s classification of adaptive compliant actuators in [22], the described system acts as a passive adaptive compliant actuator of the second type. Despite, the adaptivity is valid in a limited range determined by the non-linearity of the BC force displacement characteristic. In practice, the compliance is set by adjusting the barrel adjusters, or by setting the pre-tension during the pre-winding of the cables on the pulleys of the CBCDA.

The stiffness of the entire BCs used in Probo is tuned in such a way that the actuated joints are flexible around the desired equilibrium positions, while the positioning of these joints is still controllable without the need for extra sensory on the joints. In general the tensile strength of both materials used to construct the Bowden Cable, and the stress–strain curve determine the compliance behavior of the BC. As long as the stress is below the tensile strength, the material properties are located in the elastic region, and consequently the deformations will be canceled when the external force (or disturbance) is taken away. Without other phenomenons this leads to a repetitive behavior.

2.1.3. Bandwidth of the CBCDA

The concept bandwidth is used to indicate the response possibilities of the CBCDA. During experiments the desired position of the actuated part (joint) is following sine-waves. The amplitude A_{peak} of a sin-form equals the minimum and maximum output angle α of the joint (Fig. 11). The different amplitudes of the sine-waves were: $A_{peak} = 2\pi/3$; $2\pi/4$; $2\pi/6$; $2\pi/12$. When the sine-wave's frequency is very low, the output position can easily follow the desired positions. However, when the frequency of the sine-wave increases, the output position will have problems from a certain moment to follow the desired position due to the mechanical and the software limitations of the system. These limitations include limitations in refresh rates, acceleration and deceleration, maximum speeds, or limitations due to moments of inertia, friction, etc. In practice, the term bandwidth indicates the difference in frequencies at which the actual amplitude of the sin-wave is decreased with 3 dB compared to the desired (peak) amplitude. The gain G in dB in this scope is defined by:

$$G = 20 \cdot \log\left(\frac{A_{peak}}{A_{max}}\right) \quad (1)$$

In Eq. (1), A_{peak} equals the amplitude of the desired sine-wave to follow, and A_{max} equals the maximum amplitude that the CBCDA's output shaft (joint) has reached during an experiment. The experimental setup is presented in Fig. 12. A *CBCDA* is actuating a *Joint* over a certain distance. The position of the joint is measured by the *Encoder*. The bandwidth of two sets of Bowden cables (*Cable Set 1* and *Cable Set 2*) are determined and compared in Fig. 13.

The difference between the two graphes is devoted to the difference in stiffness of the BC sets. As one can see in Fig. 12, the BCs in *Cable Set 1* are separated. In contrast to *Cable Set 1*, the BCs in *Cable Set 2* are joined together by one heat shrink tube, only the final centimeters at the end are separated and constrained by the barrel adjusters. This setup makes the system stiffer, which results in higher bandwidths.

The bandwidths of the CBCDA-systems used to move the eyes and eyebrows of Probo are well enough to ensure smooth and natural motions over their entire range in a respectable time window.

2.1.4. Friction model

Unfortunately the use of BC introduces some difficulties to cope with. One of the drawbacks of BC based transmissions is friction. Friction can lead to significant loss in transmitted mechanical power, heat-, accuracy- and repeatability problems. Experiments were performed in order to determine the validity of a friction model based on Eq. (2). The friction model of a BC can be compared with the simplified static friction model of a rope sliding over a constrained pulley. Fig. 14 shows the model and Fig. 15 shows the experimental setup. A Bowden cable is placed between two plexi-plates in order to route the cable in two dimensions. The

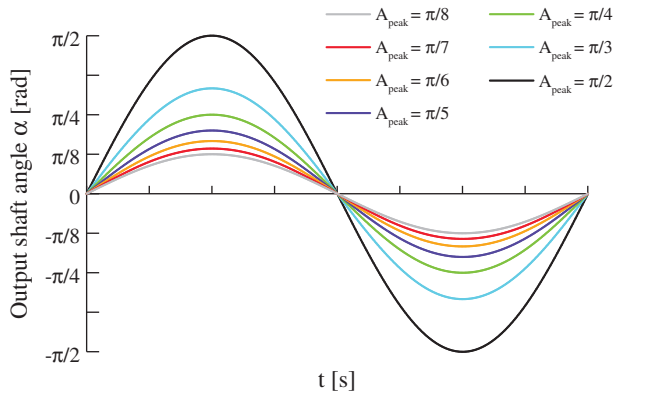

Fig. 11. The desired output angles α in function of the time. To determine the bandwidth, the frequency of the sine is increased.

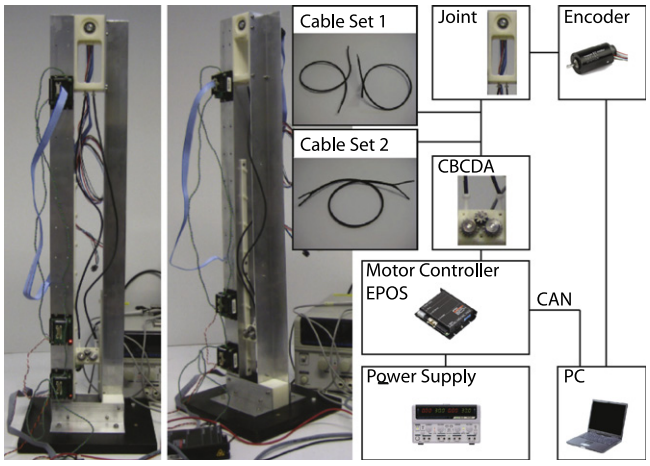

Fig. 12. Experimental setup and its schematic representation of the CBCDA actuating a joint.

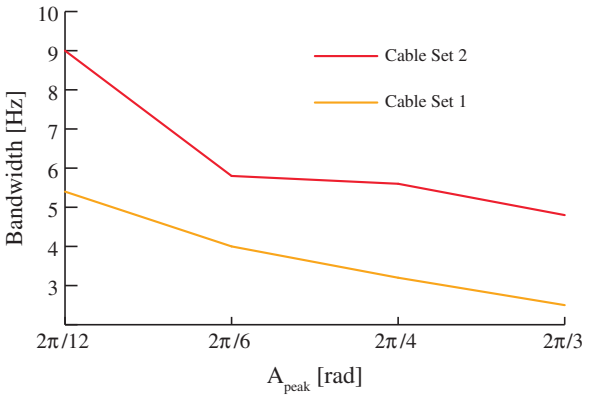

Fig. 13. Bandwidth of two different cable setups in a CBCDA actuated joint system.

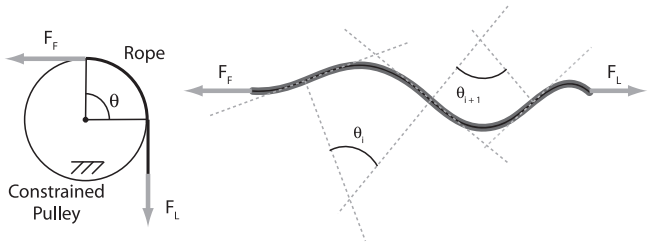

Fig. 14. Friction model Bowden cable.

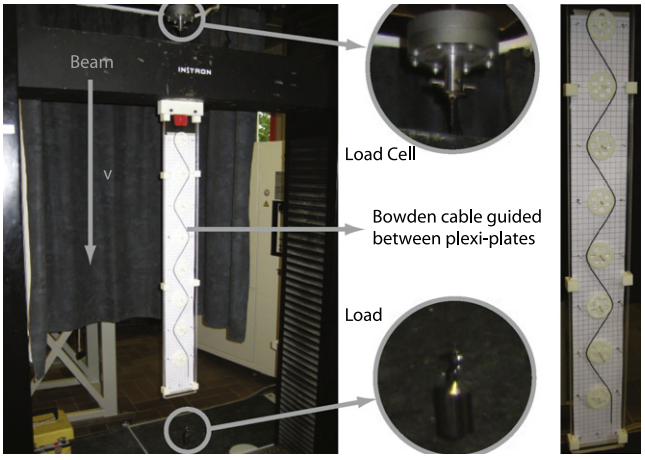

Fig. 15. Experimental setup to determine a friction model of a Bowden cable.

BC is routed with a well known span-angle since it is guided over plastic disks. The assembly of the plates which constrains the BC is mounted on the *Beam* of a pull-bench. The upper end of the inner cable of the BC, passes through the beam and is fixated to the *Load Cell*. The lower end of the inner cable is fixated to a weight (*Load*). The beam, which support the assembly of the routed BC, is movable in the vertical direction. The displacement of the beam, and the force on the *Load Cell* are measured. With this setup the relationship between the input force (determined by the mass of the weight) and the output force are measured in function of different span-angles. The total span-angle is determined by the number of disks, the radii of the disks, and the placement of the disks.

The model states that the relationship between the input and the output force is given by:

$$\frac{F_F}{F_L} = \exp^{(\mu\cdot\theta)} \tag{2}$$

In the experimental setup F_L is determined by the mass of the weight (*Load*), and F_F is measured by the *Load Cell*. Fig. 17 shows the result of a test. During this test, the inner cable was a *Fireline* cable coated with teflon, the BC sample's length was 75 mm, the speed of the beam was 5 mm/s, and the total span-angle was varying from approximately 0 to 360. For each span-angle θ, determined by a set of disks, a curve is plotted in the graph in Fig. 16. These graphes show the force F_F in function of the time. After the sticking phenomena, when F_F reaches the break-away force, the inner cable is sliding relatively through the cable housing. Then, the load cell measures a constant force. The mean value of this force F_F

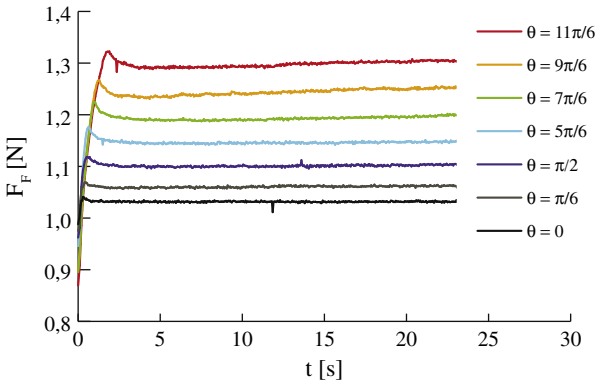

Fig. 16. Force time characteristics of a Bowden cable in function of the total span-angle when the inner cable is pulled trough its housing.

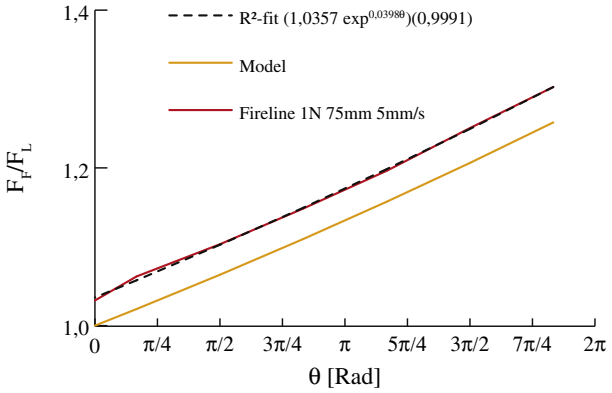

Fig. 17. Friction in function of the total span-angle.

over a certain time, together with the span-angle defines a point in the graph plotted in Fig. 17. For each curve in Fig. 16 a point can be plotted in the graph in Fig. 17.

This experiment (confirmed by other similar experiments) shows that the proposed friction model's course is followed when the model is scaled with a factor. In Fig. 17, the black line is the experimental measured curve based on the curves in 16. The dark gray line, features the curve which has the best fit to the set of data points. The coefficient of determination, R^2, is presented between brackets. In the equation determined by the curve fitting, the factor before the exponent equals the scale factor C_{exp} of this setup. The factor in the exponent before the angle θ equals the experimental friction coefficient μ_{exp} in this setup. In this experiment, the values of Eq. (3) are:

$$\frac{F_F}{F_L} = C_{exp}\cdot\exp^{(\mu_{exp}\cdot\theta)} \tag{3}$$

$$C_{exp} = 1,0357 \tag{4}$$

$$\mu_{exp} = 0,0398 \tag{5}$$

The experimental friction coefficient seems acceptable, since the rated sliding friction coefficient of teflon on teflon is about 0.04 according to different sources in the literature [33].

These kind of tests are repeated several times with different setups. For instance, the influence of the speed is presented in Fig. 18. The comparison of the curves, indicates an increase of both the correction factor C_{exp} and the experimental sliding friction coefficients μ_{exp} when the operation speed increases. The same phenomena is visible in Fig. 19, where another cable is used. Instead of the *Fireline* cable, the *Guttermann* yarn was used. The experiments show that

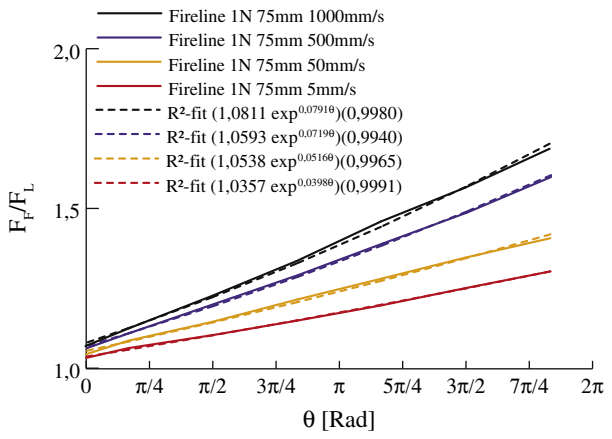

Fig. 18. Influence of speed on the friction model when Fireline cables are used.

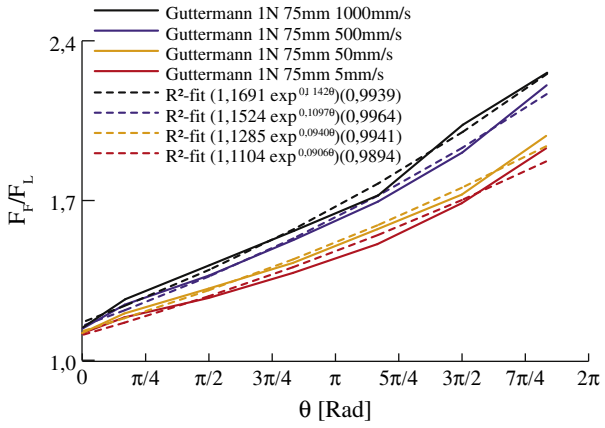

Fig. 19. Influence of speed on the friction model when Guttermann yarn is used.

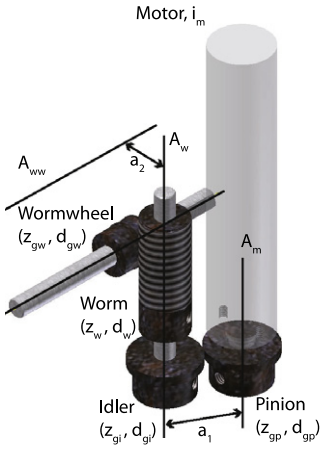

Fig. 21. Parametrization of the gears.

the sliding friction coefficient of the *Guttermann* cable is approximately twice as high as the one of the *Fireline*.

As one can see, the friction model is valid when the model is corrected with the experimental factors. When the exact efficiency of a certain setup has to be determined, or when the relationship between the input and the output force has to be known exactly, these kinds of experiments can be used to determine the behavior of the BC-system.

In the scope of Probo, it is not necessary to know the efficiency or the relationship between the input force and the output force exactly. It is roughly correct to approximate the efficiency at 50%. In general in applications that require accurate positioning on should integrate the friction model into the control algorithm of the actuator. With similar experiments a model can be made of the sticking phenomena which leads to hysteresis during positioning.

2.2. Non Back Drivable Servo (NBDS)

2.2.1. Description

The second type of the actuation systems used in the Probo prototype is referred to as *Non Back Drivable Servo (NBDS)*. The NBDS is a custom made servo motor system with a *non back drivable* gear train. Figs. 20 and 21 show some transparent views of the CAD-model to explain the working principle. A geared DC brushed *maxon* motor with incremental encoder drives an idler gear on axis A_w via a pinion gear on axis A_m (input shaft), this is the first transmission. In the second transmission, the worm on axis A_w drives the wormwheel on axis A_{ww} which is also the output shaft of the system.

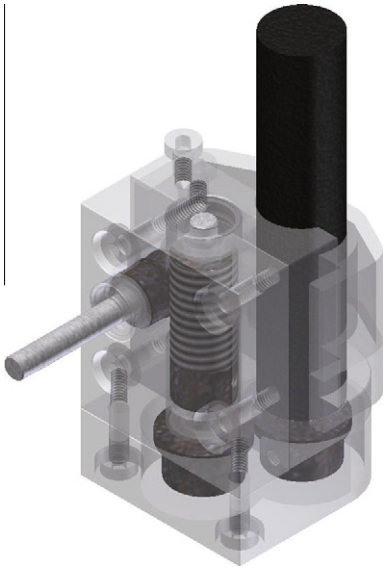

Fig. 20. A transparent view of the entire mechanism.

There are two main reasons for the first transmission. First of all it results in a compact and modular design since the driving motor can be placed parallel next to the shaft which supports the worm. The motor is only attached to the rest of the system by two screws, so it can be replaced in an easy way, without influencing the second transmission. The second reason is to allow small miss-alignment errors. When the motor-combination is used in line with axis A_w which is journalled by bearings B_1 and B_2 both axes, A_m and A_w have to be aligned perfectly otherwise the motor-shaft will slightly bend, since it is over-constrained, since the motor-shaft A_m is journalled internally in the *maxon* motor-combination. During operation it will then vibrate and harm the internal bearings, which will cause final break down. By placing the motor-combination, A_m, parallel with A_w the system is not over-constrained and small miss-alignment errors, caused by manufacturing or during assemblage, are tolerated. The distance a_1 between axes A_m and A_w can be chosen a bit larger than the ideal distance, unfortunately this will introduce more backlash in the first transmission.

The second transmission exists of the *Worm* and *Wormwheel* (Fig. 21). Unlike with ordinary gear trains, the direction of this transmission is not reversible, or also referred to as non back drivable or self-locking. In general, the property whether a worm and wormwheel will be self-locking depends on the lead angle, the pressure angle, and the coefficient of friction. However, it is approximately correct to say that a worm and wormwheel will be self-locking if the tangent of the lead angle is less than the coefficient of friction [34]. This condition is fulfilled in the NBDS. This means that the output shaft of the NBDS-system can not drive the worm, and consequently the motor-combination will not be driven either. This can be an advantage when it is used to actuate systems during HRI. It protects the internal motor-combinations by eliminating any possibility of the output driving the input. The main disadvantage is the loss in transmitted power due to the friction. This can be noticed in the rather small efficiency in comparison with other transmission (typically 50%).

2.2.2. Compliance of the NBDS

The NBDS is non-backdrivable to protect the internal motor-combinations by eliminating any possibility of the output driving the input. This is interesting when children physically interact with

Fig. 22. An overview of the ear-system.

the robot. This also means there is no compliance at this moment in the actuator. To introduce the huggable aspect this NBDS drives a flexible part of the body. For example, the basic ideas to introduce the compliance in the ear-system are visible in Fig. 22. The two NBDSs are used to actuate the ears. As one can see, they are each others mirror image. The ear itself is a helical spring. This spring is fixated with one end to the output shaft of its actuating NBDS, while the other end can be moved freely around its axial centerline. A flexible foam core in the shape of the ear is then placed over the spring. When the NBDS's output shaft is turning, it will rotate the constrained foam ear.

The same type of actuator (variant of the NBDS) and the same ideas to introduce the compliance are used in Probo's trunk-system (Fig. 23). Probo's trunk has three combined DOFs. The main parts in the system are the *foam core* trunk itself, the *flexible cables*, and the *NBDSs*. This core consists of ten discs. These discs are constrained to the axial centerline of the core. Through the discs, parallel to the centerline of the core, three flexible cables are guided through hollow bushes. These hollow bushes are constrained to the discs. Since the trunk's core and cables are flexible, the trunk-system is flexible and gives a safe and huggable characteristic.

In order to obtain Probo's final shape and appearance, the internal robotic hardware is covered. The covering exists of different layers. Hard ABS covers shield and protect Probo's internal hardware. These covers are fixated to the head- and body-frames at the different points. The covers roughly define the shape of Probo. These are manufactured by use of rapid prototyping techniques, which means that the parts are built layer by layer. These covers are encapsulated in a PUR foam layer, that is covered with a removable fur-jacket. The fur-jacket can be washed and disinfected, and complies to the European toy safety standards EN71-1, EN71-2 and EN71-3. The use of the soft actuation principle together with well-

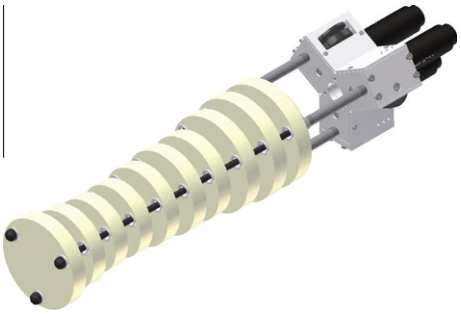

Fig. 23. An overview of the trunk-system.

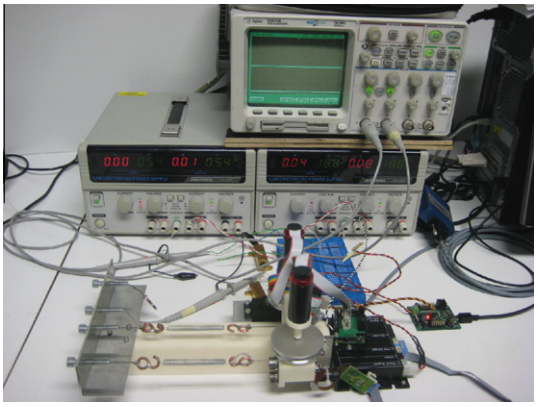

Fig. 25. Experimental set up to compare NBDS with HS5745MG.

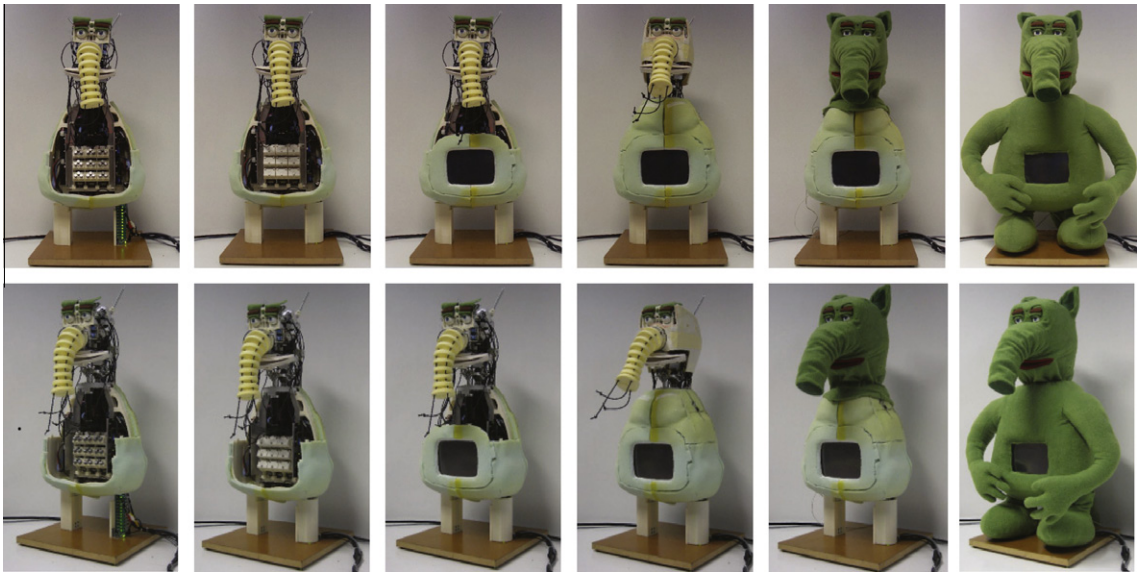

Fig. 24. Probo from robot to huggable animal.

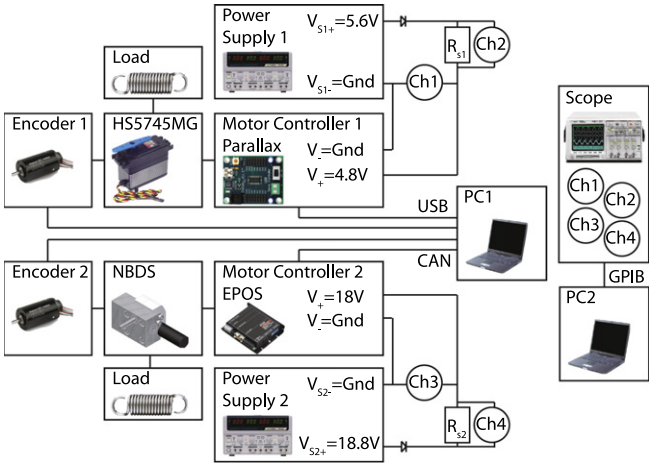

Fig. 26. Schematic representation of the experimental set up.

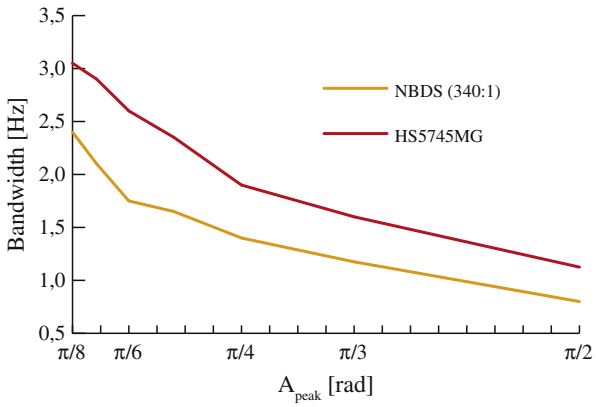

Fig. 27. Bandwidth of the NBDS (340:1) and the HS5745MG for varying amplitudes of the sine-wave.

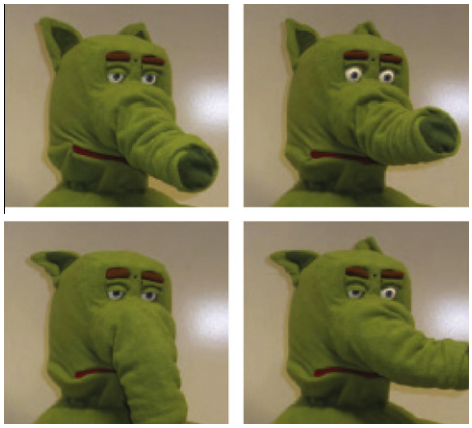

Fig. 28. Facial expressions mechanically rendered by use of CBCDAs and NBDSs.

Fig. 29. The prototype of the huggable robot Probo interacting with children.

thought designs concerning the robot's filling and huggable fur, are both essential to create Probo's soft touch feeling and ensure safe interaction. A chronological way how the robotic Probo becomes huggable is presented in Fig. 24.

2.2.3. Bandwidth of the NBDS

Analogue to the bandwidth tests described in Section 2.1.3, a similar test is set up to determine the NBDS's bandwidth. The experimental setup is presented in Figs. 25 and 26. With this setup it is possible to test and compare the NBDS with a regular servo. The *Load* of the systems can be chosen by the placement of pull springs with certain force displacement characteristics whether or not in an antagonistic setup. The positions of the systems' output-shafts are measured by *Encoder 1* and *Encoder 2*. The supply voltage and the current of the motor driver units are measured by the *Scope*. The data acquisition of the measured position, current and voltage during an experiment is done by *PC 1* and *PC 2*. Furthermore, *PC 1* communicates with the lower level motor-controllers, which control the servos. This setup is, among other tests, used to determine the mechanical bandwidth of the NBDS with a total transmission ratio of 340:1 and the *Hitec HS5745MG RC* servo.

The resulting bandwidths are presented and compared with those of the RC servo in Fig. 27. As one can see, the bandwidths of the RC servo are slightly higher than the corresponding ones of the NBDS. This is devoted to the higher speeds according to their speed-torque characteristics. However, the acceleration, deceleration and speeds are determined by the load as well. In the described experiments the servos were unloaded. Similar bandwidth tests can be done with different loads, in order to determine the influence.

The bandwidths of the NBDS systems used to move the ears and the mouth corners of Probo are well enough to ensure smooth and natural motions over their entire range in a respectable time window.

3. Validation of Probo's actuators

The CBCDA as well as the NBDS in combination with the fur covered flexible parts foresee in the demands of the Probo project. These actuators make it possible to render mechanically facial expressions and to change these expressions within a respectable time window so that Probo's behavior seems natural. The accuracy of positioning is high enough to clearly differentiate facial expressions which lead to certain emotional communication. Some of Probo's facial expressions are shown in Fig. 28. According to other work of the authors, the covering of Probo not only contributes to its child-friendly appearance, it also increases the level of emotional communication during face-to-face encounters [35]. The Probo prototype has been demonstrated at several public events (Fig. 29) all over the world and in general people's reactions were very positive. After hundreds of hours of operating, the facial expressions were still recognizable, and the positioning did not shift significantly, which proves that the actuated systems are quite repetitive as well. The accompanying video shows the working principle of the two presented actuators and how they are

implemented in the robot Probo. The compliance of the different actuated joints is presented as well.

4. Conclusion

The mechanical design process of Probo aimed to develop a social robot with a huggable and safe behavior. Probo's soft touch is introduced, on the one side by use of novel passive compliant actuators, Compliant Bowden Cable Driven Actuators (CBCDAs), and on the other side by combining custom made servo motors, Non Back Drivable Servos (NBDSs), with flexible components and materials such as springs, silicon and foam. The two custom made actuators' working principle and the parameters to determine the systems' specifications are explained. The CBCDA is developed so the motor can be placed on a remote location (e.g., the body) to reduce the weight of the moving part. Experimental setups and tests are presented to determine the bandwidth of the CBCDA, and the stiffness characteristics and friction model of the Bowden Cables (BC). One can increase the bandwidth of a CBCDA by increasing the stiffness of the BCs. The stiffness of the BC is determined by the tensile strengths and stress–strain curves of the BCs' materials. The friction model follows the slope of the model of a rope sliding over a constraint pulley. It depends on the friction coefficient of the materials, the span angle and an experimental correction factor. In applications where relative large powers have to be transmitted, the friction model should be integrated in the control algorithm, as well as the sticking phenomena. In order to adapt the CBCDA from a passive compliant actuator to an adjustable (and active) compliant actuator, one can opt to automate the process of pre-winding the BCs or change the pre-tension by use of an extra linear or rotational actuator. The NBDS is developed to protect the internal motor-combinations by eliminating any possibility of the output driving the input. An experimental setup to test and compare the custom made servo with regular commercial servos is presented. In spite the lack of analytical prove, both types of actuators fulfill the needs of actuators for Probo, and prove their accuracy, repeatability and durability. For now, the achievement of the huggable behavior by use of these actuators is measured in a subjective way based on the feelings and reactions of children and people interacting with Probo. In the future, specific tests must be set up in collaboration with psychologists to measure perception and to translate it into engineer-friendly metrical parameters. Nonetheless, the ideas behind the concepts themselves and the experiments to determine their main parameters and validation, may give some insights in the design of other similar actuators and/or applications.

Acknowledgments

This work has been funded by the Brussels Capital Region, Belgium, and by the European Commissions 7th Framework Program as part of the project VIACTORS under Grant No. 231554.

Appendix A. Supplementary data

Supplementary data associated with this article can be found, in the online version, at doi:10.1016/j.mechatronics.2011.01.001.

References

[1] Mehrabian A. Communication without words. Psychol Today 1968;2(4):53–6.
[2] Ortony A, Norman D, Revelle W. 7 Affect and proto-affect in effective functioning, Who Needs Emotions?: The Brain Meets the Robot; 2005.
[3] Canamero L, Fredslund J. How does it feel? emotional interaction with a humanoid lego robot. Socially intelligent agents: the human in the loop. Papers from the AAAI 2000 fall symposium; 2000. p. 23–8.
[4] van Breemen A. iCat: experimenting with animabotics. In: Proceedings, AISB 2005 creative robotics symposium; 2005.
[5] Breazeal C. Designing sociable robots. Mit Pr; 2002.
[6] W. MIT Media Lab. Personal robots group; 2009. <http://robotic.media.mit.edu/>.
[7] Kozima H. Infanoid: an experimental tool for developmental psycho-robotics. In: International workshop on developmental study. Citeseer; 2000.
[8] Dautenhahn K, Nehaniv C, Walters M, Robins B, Kose-Bagci H, Mirza N, et al. KASPAR – a minimally expressive humanoid robot for human–robot interaction research.
[9] Mitsunaga N, Miyashita T, Ishiguro H, Kogure K, Hagita N. Robovie-iv: a communication robot interacting with people daily in an office. In: IEEE/RSJ international conference on intelligent robots and systems; 2006. p. 5066–72.
[10] Hertenstein M, Verkamp J, Kerestes A, Holmes R. The communicative functions of touch in humans, nonhuman primates, and rats: a review and synthesis of the empirical research. Genetic Soc General Psychol Monogr 2006;132(1):5–94.
[11] Alonso J, Chang A, Robots P, Orkin J, Machines C, Breazeal C. Eliciting collaborative social interactions via online games.
[12] Sakagami Y, Watanabe R, Aoyama C, Matsunaga S, Higaki N, Fujimura K, et al. The intelligent ASIMO: system overview and integration. In: IEEE/RSJ international conference on intelligent robots and system, vol. 3; 2002.
[13] Sawada T, Takagi T, Fujita M. Behavior selection and motion modulation in emotionally grounded architecture for QRIO SDR-4XII. In: 2004 IEEE/RSJ international conference on intelligent robots and systems, 2004.(IROS 2004). Proceedings, vol. 3.
[14] Zecca M, Endo N, Momoki S, Itoh K, Takanishi A. Design of the humanoid robot KOBIAN: preliminary analysis of facial and whole body emotion expression capabilities. In: Proceedings of 2008 IEEE-RAS 8th international conference on humanoid robots; 2008. p. 487–92.
[15] Metta G, Sandini G, Vernon D, Natale L, Nori F. The iCub humanoid robot: an open platform for research in embodied cognition. In: Proceedings of IEEE workshop on performance metrics for intelligent systems workshop. ACM; 2008.
[16] Wada K, Shibata T, Saito T, Tanie K. Analysis of factors that bring mental effects to elderly people in robot assisted activity. In: IEEE/RSJ international conference on intelligent robots and system, 2002, vol. 2; 2002.
[17] Billard A, Robins B, Nadel J, Dautenhahn K. Building robota, a mini-humanoid robot for the rehabilitation of children with autism. RESNA Assistive Technol J 2006.
[18] Stiehl W, Lieberman J, Breazeal C, Basel L, Lalla L, Wolf M. Design of a therapeutic robotic companion for relational, affective touch. Robot and human interactive communication, 2005. ROMAN 2005. IEEE International Workshop on; 2005. p. 408–15.
[19] Fujita M. AIBO: toward the era of digital creatures. Int J Robot Res 2001;20(10):781.
[20] Stiehl W, Breazeal C. Affective touch for robotic companions. In: First international conference on affective computing and intelligent interaction (currently under review). Springer; 2005.
[21] Van Damme M, Vanderborght B, Verrelst B, Van Ham R, Daerden F, Lefeber D. Proxy-based sliding mode control of a planar pneumatic manipulator. Int J Robot Res 2009;28(2):266–84.
[22] Ham R, Sugar T, Vanderborght B, Hollander K, Lefeber D. Compliant actuator designs: review of actuators with passive adjustable compliance/controllable stiffness for robotic applications. IEEE Robot Autom Mag 2009;16(3):81–94.
[23] Pratt G, Williamson M. Series elastic actuators. In: Proceedings of the IEEE/RSJ international conference on intelligent robots and systems (IROS-95), vol. 1; 1995. p. 399–406.
[24] Verrelst B, Ham R, Vanderborght B, Daerden F, Lefeber D, Vermeulen J. The pneumatic biped lucy actuated with pleated pneumatic artificial muscles. Auton Robots 2005;18(2):201–13.
[25] Tonietti G, Schiavi R, Bicchi A. Design and control of a variable stiffness actuator for safe and fast physical human/robot interaction. In: Proceedings of 2005 IEEE international conference on robotics and automation; 2005. p. 526–31.
[26] Hollander K, Sugar T, Herring D. Adjustable robotic tendon using a jack spring. In: Proceedings of 2005 IEEE 9th international conference on rehabilitation robotics; 2005. p. 113–8.
[27] Van Ham R, Vanderborght B, Van Damme M, Verrelst B, Lefeber D. MACCEPA, the mechanically adjustable compliance and controllable equilibrium position actuator: design and implementation in a biped robot. Robot Auton Syst 2007;55 (10):761–8.
[28] Haddadin S, Albu-Schäffer A, Hirzinger G. Int J Robot Res.
[29] Hollerbach J, Hunter I, Ballantyne J. A comparative analysis of actuator technologies for robotics. Robot Rev 1992;2:299–342.
[30] Selden B, Cho K, Asada H. Segmented shape memory alloy actuators using hysteresis loop control. Smart Mater Struct 2006;15(2):642–52.
[31] Cho M, Seo H, Nam J, Choi H, Koo J, Song K, et al. A solid state actuator based on the PEDOT/NBR system. Sensors Actuat B: Chem 2006;119(2):621–4.
[32] W. Scientific Commodities. Scientific commodities incorporated; 2009. <http://www.scicominc.com/>.
[33] Serway R, Beichner R, Jewett J. Physics for scientists and engineers with modern physics. Saunders College Publishers; 2000.
[34] Muhs D, Wittel H, Becker M, Jannasch D. Roloff/matek machine onderdelen: normering, berekening, vormgeving. Academic Service, Schoonhoven; 2000.
[35] Saldien J, Goris K, Vanderborght B, Vanderfaeillie J, Lefeber D. Expressing emotions with the social robot probo. Int J Soc Robot 1–13.